Title
Charged iron particles, components of space radiation, destroy ovarian follicles

Journal
Human Reproduction, 31(8)

ISSN
0268-1161

Authors
Mishra, Birendra
Ortiz, Laura
Luderer, Ulrike

Publication Date
2016-08-01

DOI
10.1093/humrep/dew126

Peer reviewed

Human Reproduction, Vol.31, No.8 pp. 1816–1826, 2016
Advanced Access publication on May 31, 2016 doi:10.1093/humrep/dew126

human reproduction

ORIGINAL ARTICLE *Reproductive biology*

Charged iron particles, components of space radiation, destroy ovarian follicles

Birendra Mishra[1], Laura Ortiz[1], and Ulrike Luderer[1,2,3,*]

[1]Department of Medicine, University of California Irvine, Irvine, CA 92617, USA [2]Developmental and Cell Biology, University of California Irvine, Irvine, CA 92617, USA [3]Program in Public Health, University of California Irvine, Irvine, CA 92617, USA

*Correspondence address. Center for Occupational and Environmental Health, 100 Theory Drive, Suite 100, Irvine, CA 92617, USA. Tel: +1-949-824-8641; Fax: +1-949-824-2345; E-mail: uluderer@uci.edu

Submitted on January 9, 2016; resubmitted on May 5, 2016; accepted on May 11, 2016

STUDY QUESTION: Do charged iron particles, components of space radiation, cause premature ovarian failure?

SUMMARY ANSWER: Exposure to charged iron particles causes ovarian DNA damage, oxidative damage and apoptosis, resulting in premature ovarian failure.

WHAT IS KNOWN ALREADY: The ovary is very sensitive to follicle destruction by low linear energy transfer (LET) radiation, such as X-rays and γ-rays. However, it is completely unknown whether high-LET radiation, such as charged iron particles, also destroys ovarian follicles.

STUDY DESIGN, SIZE, DURATION: Twelve week old C57BL/6J female mice were exposed to single doses of 0, 5, 30 or 50 cGy ($n = 8$/group) charged iron particles (LET = 179 keV/μm) at energy of 600 MeV/u. Two groups were irradiated at the highest dose, one fed AIN-93M chow and the other fed AIN-93M chow supplemented with 150 mg/kg diet alpha lipoic acid (ALA).

PARTICIPANTS/MATERIALS, SETTING, METHODS: We quantified the numbers of ovarian follicles, measured serum follicle stimulating hormone (FSH) and luteinizing hormone (LH) concentrations, and analyzed histone H2AX phosphorylation, oxidative damage and apoptosis markers in the ovarian follicles.

MAIN RESULTS AND THE ROLE OF CHANCE: H2AX phosphorylation, lipid peroxidation, protein nitration and apoptosis were highly induced in ovarian follicles at 6 h and remained increased 1 week after irradiation. As a result, numbers of healthy ovarian follicles were significantly and dose-dependently depleted at 1 and 8 weeks post-irradiation, with 57, 84 and 99% decreases in primordial follicles at 8 weeks at the 5, 30 and 50 cGy doses, respectively ($P < 0.05$ versus 0 cGy). Consistent with near-total depletion of ovarian follicles in the 50 cGy group, serum concentrations of FSH and LH were significantly elevated at 8 weeks. Dietary supplementation with ALA partially prevented the adverse ovarian effects of 50 cGy iron particles.

LIMITATIONS, REASONS FOR CAUTION: About 21% of the estimated radiation dose from exposure to galactic cosmic rays during a multi-year Mars mission will be due to high-LET particles, of which iron is only one. The effects of galactic cosmic rays, which contain a mixture of multiple charged particles, as well as protons, neutrons, and helium ions, may differ from the effects of iron alone.

WIDER IMPLICATIONS OF THE FINDINGS: We show for the first time that charged high-LET ions are highly damaging to the ovary even at low doses, causing premature ovarian failure. In addition to raising concerns for female astronauts, these findings raise concerns for ovarian damage due to clinical uses of high-LET particles for cancer treatment. In addition to causing infertility, premature ovarian failure has adverse implications for the functions of heart, brain, bone and muscle later in life.

STUDY FUNDING/COMPETING INTEREST(S): This work was supported by a National Aeronautics and Space Administration grant NNX14AC50G to U.L. B.M. was partially supported by a National Space Biomedical Research Institute First Award, PF04302. Additional support was received from the University of California Irvine Center for Occupational and Environmental Health. The authors have no conflicts of interests.

Key words: charged particles / ionizing radiation / ovarian follicle / premature ovarian failure / apoptosis / oxidative stress

Introduction

Female mammals are born with a finite supply of oocytes, which declines continuously throughout reproductive life, culminating in reproductive senescence, termed menopause in humans. Prior to menopause, quiescent primordial follicles are continuously recruited into the growing pool and pass through primary, secondary, antral, and, finally, pre-ovulatory stages of growth to ovulate oocytes. However, more than 95% of

these follicles undergo apoptotic degeneration (atresia) before reaching the pre-ovulatory follicle stage (Gosden *et al.*, 1983; Hirshfield, 1988, 1997). The rate of follicle depletion can be accelerated by exposure to environmental toxicants, chemotherapeutic agents or ionizing radiation (Devine *et al.*, 2012; Lee *et al.*, 2000; Meirow and Nugent, 2001; Wallace *et al.*, 1989, 2003), leading to early onset of ovarian senescence.

The ovary is highly sensitive to γ-radiation. Gamma radiation destroys follicles at all stages of growth (Kim and Lee, 2000; Lee *et al.*, 2000; Lee and Yoon, 2005); however, primordial stage follicles appear to be most sensitive (Kerr *et al.*, 2012). Once the reserve of primordial follicles is depleted, ovarian failure ensues. Premature ovarian failure has many adverse consequences, including early loss of fertility and increased risk of osteoporosis, cardiovascular disease and Alzheimer's disease (Molina *et al.*, 2005; Shuster *et al.*, 2008; Silva *et al.*, 2001; Svejme *et al.*, 2012). Germ cell depletion is also hypothesized to play a role in the pathophysiology of ovarian cancer (Capen *et al.*, 1995; Vanderhyden *et al.*, 2003). Accumulating evidence supports a role for oxidative stress in normal and premature ovarian aging (Devine *et al.*, 2012; Lim *et al.*, 2013, 2015). Our own and others' work has shown that γ-irradiation chronically elevates cellular reactive oxygen species (ROS) production and oxidative stress and that ROS initiate apoptotic death of ovarian follicles (Spitz *et al.*, 2004; Tsai-Turton and Luderer, 2006; Tsai-Turton *et al.*, 2007; Dayal *et al.*, 2008; Cortés-Wanstreet *et al.*, 2009).

Women made up half of the 2013 National Aeronautics and Space Administration (NASA) astronaut class (Ronca *et al.*, 2014). During space missions, astronauts are exposed to galactic cosmic rays, which contain protons, neutrons, helium ions and ions heavier than helium. It is estimated that astronauts will be exposed to 40 cGy absorbed dose (1.07 Sv effective dose) of ionizing radiation during the anticipated 3 year duration of a Mars mission (Cucinotta and Durante, 2006; Barcellus-Hoff *et al.*, 2015). Approximately 21% of the ionizing dose equivalent comes from the high charge and energy (HZE) particles (Slaba *et al.*, 2015). HZE particles have high-linear energy transfer (LET), as compared with low LET X-rays and γ-rays. High-LET radiation is thought to be more destructive to cells than low LET radiation for a given dose, but this depends to some extent on the end-point being examined, as well as on the energy, charge and velocity of the particles (Sridharan *et al.*, 2015; Tokuyama *et al.*, 2015). Charged particles, such as carbon ions and protons, are also increasingly being used for cancer treatment (Loeffler and Durante, 2012).

Despite these clinical uses and concern about chronic health effects in female astronauts, the effects of charged particle radiation on the ovary have received minimal attention. To begin to address this data gap, we analyzed the ovarian effects of low-dose irradiation with charged iron particles. We hypothesized that exposure to charged iron particles causes DNA damage, oxidative stress and apoptosis in ovarian follicles, resulting in premature ovarian failure.

Materials and Methods

Animals

Twelve week old female mice (C57BL/6J from Jackson Labs, $n = 8$/experimental group) were exposed to 0, 5, 30 or 50 cGy charged iron particles (LET = 179 keV/μm) at energy of 600 MeV/u and dose rates of 13.5–18.6 cGy/min. Two groups were irradiated at the highest dose, one fed AIN-93M chow and the other fed the same chow supplemented with 150 mg/kg diet of the antioxidant ALA (Bio-Serv, Flemington, NJ, USA), beginning 1 week before irradiation and continuing until euthanasia. Irradiations were performed at the NASA Space Radiation Laboratory, Brookhaven National Laboratory, NY, USA. Mice for the 0 cGy group were transported and restrained identically to the irradiated groups. All animal procedures were approved by the Institutional Animal Care and Use Committees at Brookhaven National Laboratory and University of California Irvine. Mice were euthanized by CO_2 inhalation at 6 h and 1 week after irradiation and on the metestrous stage of the estrous cycle, determined by vaginal cytology, at ~8 weeks after irradiation. Ovaries and blood were collected at the time of euthanasia.

Vaginal cytology

Estrous cycling was monitored every morning by the microscopic examination of fresh vaginal lavage fluid obtained in 0.9% sodium chloride (Cooper *et al.*, 1993) beginning at 6 weeks after irradiation and continuing for at least 3 estrous cycles or 14 days if the mice were not cycling. Mice were housed individually for 1 week before and while monitoring estrous cycles and were euthanized by CO_2 inhalation on the day of metestrus of the estrous cycle at approximately 8 weeks after irradiation. Estrous cycles were not monitored in the 6 h and 1 week time point mice for these acute time points because we deemed it more important to euthanize the mice as close to the designated time point as possible.

Ovarian histomorphometric analysis

Ovaries were fixed in Bouin's fixative, washed in 50% ethanol four times, and stored in 70% ethanol until they were embedded in paraffin. Ovaries were then serially sectioned at 5 μm thickness all the way through the entire tissue. Sections were stained with hematoxylin and eosin. Ovarian follicles were counted using light microscopy, blind to the treatment group. Ovarian follicles were classified as primordial (oocytes with single layer of flattened granulosa cells), primary (oocytes with single layer of cuboidal or mixed cuboidal/flattened granulosa cells), secondary (oocytes with more than one layer of granulosa cells) or antral (oocytes with multiple layers of granulosa cells and possessing an antral space or spaces) and were further classified as healthy or atretic as described previously (Lopez and Luderer, 2004; Lim *et al.*, 2013). Atretic secondary and antral follicles were identified by the presence of three or more pyknotic granulosa cells per largest cross-section and separation of the oocyte from the granulosa cells. Atretic primordial and primary follicles were identified by eosinophilic oocytes. Primordial, primary and secondary follicles were counted in every fifth serial section. The counts were multiplied five times to obtain estimates of the total number of follicles per ovary. To avoid overcounting, primordial and small primary follicles were only counted if the oocyte nucleus was clearly visible, and larger primary and secondary follicles were only counted if the oocyte nucleolus was clearly visible (Canning *et al.*, 2002). Antral follicles were followed through every section taking care to count each antral follicle only once.

Immunohistochemical analysis

Paraformaldehyde-fixed, OCT embedded ovaries were serially sectioned at 7 μm thickness and slides were stored at −80°C. Slides were subjected to antigen retrieval using 10 mmol/l sodium citrate with 0.05% Tween-20 at 95°C, blocked with avidin and biotin blocking reagents and normal goat serum, and incubated with primary antibodies to phosphorylated histone 2AX (γH2AX), 4-hydroxynonenal (4-HNE), nitrotyrosine (NTY), activated caspase 3, p53 up-regulated modulator of apoptosis (PUMA) or proliferating cell nuclear antigen (PCNA), then a secondary antibody as detailed in Supplementary data, Table SI. Sections were then blocked with 0.3% H_20_2 and incubated with ABC reagent (Vector Laboratories), and immunostaining was visualized with diaminobenzidine substrate in peroxide buffer (Roche).

Sections were counterstained with hematoxylin. The following negative controls were included in each immunostaining run: (i) primary antibody without secondary antibody, (ii) primary antibody replaced by nonimmune IgG with secondary antibody, (iii) secondary antibody without primary antibody.

Scoring of immunostaining was done blind to treatment group. Primordial and primary follicles containing one or more positive granulosa cells, secondary follicles containing two or more positive granulosa cells or theca cells, and antral follicles containing three or more positive granulosa cells or theca cells were considered positive. In addition, oocytes were also scored as positive or negative. The percentage of positive follicles or oocytes per section was calculated. Two separate immunostaining runs consisting of one slide per ovary with four sections each were performed for each end-point, and the percentages from the eight scored sections per ovary were averaged for analysis.

Measurement of hormones

Serum concentrations of follicle stimulating hormone (FSH) and luteinizing hormone (LH) were measured using Millipore Pituitary Panel Multiplex kits at the Center for Research in Reproduction, University of Virginia, Charlottesville, VA, USA. The intra- and inter-assay coefficients of variation for these assays were 5.5 and 11.5%, respectively.

Statistical analyses

All data are presented as the mean ± SEM in figures. Differences among treatment groups were analyzed by analysis of variance (ANOVA) followed by post hoc LSD or Dunnett T3 test for follicle counts or hormone concentrations. Differences among groups for end-points expressed as percentages were analyzed by nonparametric Kruskal–Wallis test followed by Mann–Whitney *U* test. Statistical analyses were carried out using SPSS 20 (Windows) or SPSS 23 (Macintosh; IBM Corporation).

Results

Charged iron particles deplete ovarian follicles

One week after irradiation, the numbers of healthy primordial ($P < 0.001$, effect of group), primary ($P < 0.001$), secondary ($P < 0.001$) and antral ($P = 0.006$) follicles per ovary were dose-dependently decreased in mice irradiated with iron compared with 0 cGy controls (Fig. 1). Intergroup comparisons revealed statistically significant differences in primordial, primary and antral follicles between the 30 and 50 cGy groups and the 0 cGy group. The ALA supplemented diet significantly mitigated the decline in the number of primordial follicles caused by exposure to 50 cGy iron at 1 week. At 8 weeks after irradiation, statistically significant differences among groups were observed in primordial ($P < 0.001$), primary ($P < 0.001$), secondary ($P = 0.001$) and antral follicle numbers ($P = 0.011$; Fig. 1). Intergroup comparisons revealed that primordial follicles were significantly decreased relative to controls by all three doses, with a 57% decline in primordial follicle numbers in the 5 cGy group.

At 8 weeks, 12.5 and 25%, respectively, of mice treated with 50 cGy charged iron or 50 cGy iron plus ALA had irregular estrous cycles compared with 0% of the other groups (data not shown, differences not statistically significant). Mice treated with 50 cGy iron had nonsignificantly longer estrous cycles than controls (5.2 ± 0.3 days versus 4.3 ± 0.2 days in controls).

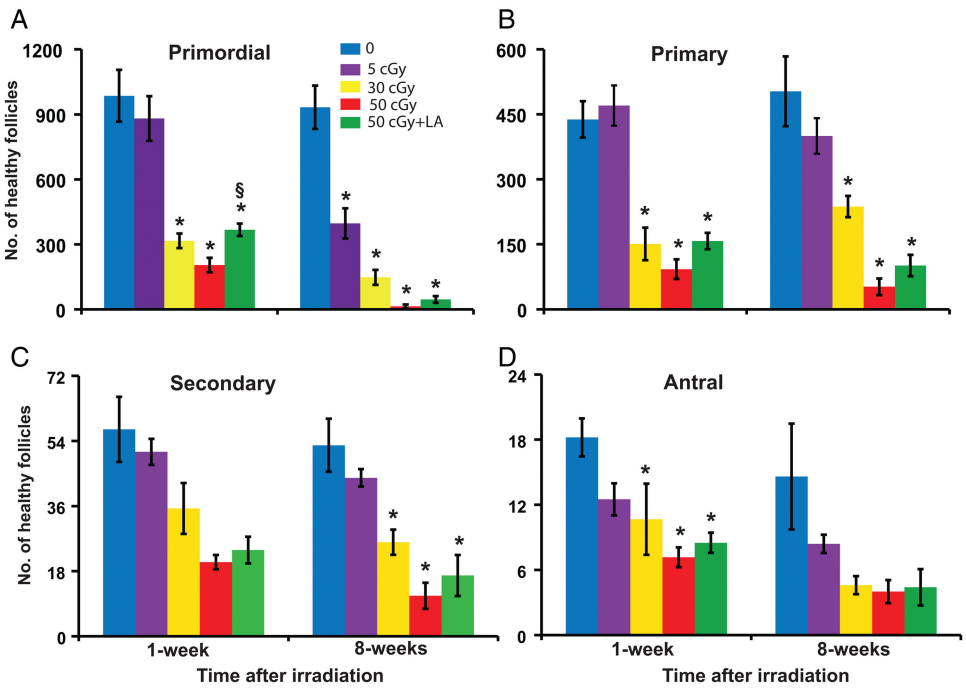

Figure 1 Charged iron particles deplete ovarian follicles. Mice in this and subsequent figures were fed normal diet or diet supplemented with 150 mg/kg ALA from 1 week before irradiation with the indicated doses of charged iron particles until euthanasia. Graphs show the mean ± SEM of healthy follicles of the indicated stages of development per ovary. (**A**) Primordial follicles, $P < 0.001$, effect of group by ANOVA at both time points. (**B**) Primary follicles, $P < 0.001$, effect of group by ANOVA at both time points. (**C**) Secondary follicles, $P \leq 0.001$, effect of group by ANOVA at both time points. (**D**) Antral follicles $P \leq 0.011$, effect of group by ANOVA at both time points. *$P < 0.05$, compared with 0 cGy control; $^{\S}P < 0.05$, 50 cGY + ALA compared with 50 cGy. $n = 5–6$/group.

Charged iron particles alter reproductive hormone concentrations

At 8 weeks post-irradiation, serum FSH and LH concentrations increased with charged iron particle dose ($P < 0.001$ and $P = 0.016$, respectively, effects of treatment group; Fig. 2A and B). Mice irradiated with 50 cGy iron plus the ALA supplemented diet had similar levels of FSH and LH as the 50 cGy iron group on the nonsupplemented diet (Fig. 2A and B).

Charged iron particles increase ovarian histone 2AX phosphorylation

We analyzed immunostaining for γH2AX, a marker of DNA double strand breaks, in ovarian sections 6 h and 1 week post-irradiation from the 0, 50, and 50 cGy plus ALA groups (Fig. 3). At 6 h, the percentages of secondary and antral follicles with γH2AX-positive granulosa cells were significantly higher in 50 cGy exposed mice compared with 0 cGy controls ($P < 0.05$), whereas 50 cGy iron plus ALA treated mice had significantly decreased percentages of γH2AX immunostained secondary and antral follicles compared with 50 cGy iron treated mice ($^{\S}P < 0.05$ relative to 50 cGy; Fig. 3C). At 6 h, the percentages of primordial, primary and secondary follicles with γH2AX-positive oocytes were significantly higher in mice exposed to 50 cGy iron relative to controls ($P < 0.05$), whereas ALA-supplemented 50 cGy-treated mice had similar levels of oocyte γH2AX immunostaining as controls (Fig. 3D). At 1 week after irradiation, the percentages of secondary and antral follicles with γH2AX-positive granulosa cells were significantly higher in 50 cGy versus control mice ($P < 0.05$), and these effects were mitigated by ALA supplementation (Fig. 3E). However, no statistically significant differences in the percentages of γH2AX-positive oocytes remained at 1 week (Fig. 3F).

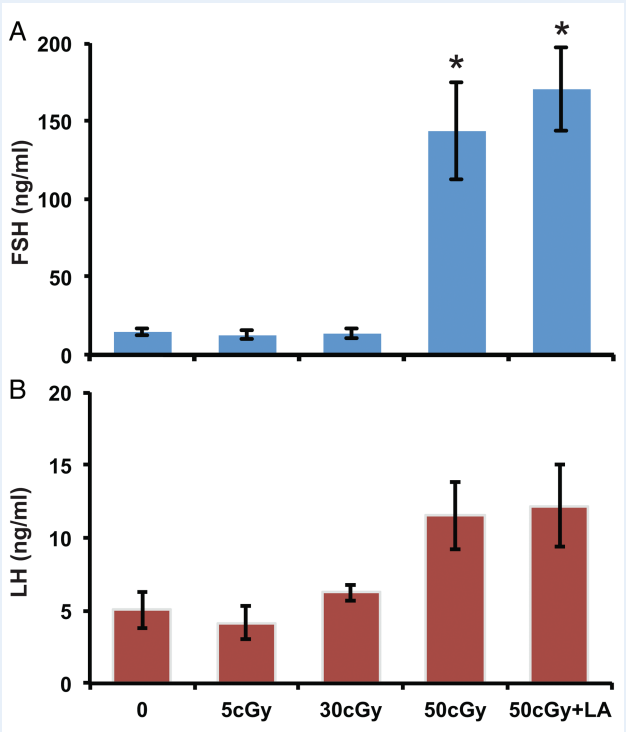

Figure 2 Charged iron particles decrease ovarian negative feedback to the hypothalamus and pituitary. Graphs show the mean ± SEM of serum FSH or LH levels at 8 weeks after irradiation. (**A**) There were significant differences in FSH concentrations among treatment groups ($P < 0.001$). (**B**) There were significant differences in LH concentrations among treatment groups ($P = 0.016$). *$P < 0.05$, compared with 0 cGy control. $n = 5–8$ mice/group.

Charged iron particles increase ovarian oxidative stress

To test whether iron charged particles induce oxidative stress in the ovary, we performed immunostaining with antibodies for a marker of lipid peroxidation, 4-HNE (Roede and Jones, 2010) and a marker of protein oxidation, NTY; (Radi, 2013; Reeg and Grune, 2015) in ovaries from the 0, 50, and 50 cGy plus ALA groups (Figs 4 and 5).

At 6 h after irradiation, the percentage of secondary follicles with 4-HNE-positive granulosa cells was significantly higher in 50 cGy exposed mice compared with 0 cGy controls ($P < 0.05$), and these effects were mitigated by ALA supplementation ($^{\S}P < 0.05$; Fig. 4C). At 6 h the percentages of follicles with 4-HNE-positive oocytes were significantly higher for primordial, primary and secondary follicles in mice exposed to 50 cGy iron relative to controls ($P < 0.05$), whereas mice that received 50 cGy iron plus ALA had similar levels of oocyte 4-HNE immunostaining as controls (Fig. 4D). At 1 week after irradiation, the percentages of primary, secondary and antral follicles with 4-HNE positive granulosa cells (Fig. 4E) and the percentages of primordial, primary, secondary and antral follicles with 4-HNE positive oocytes (Fig. 4F) were significantly higher in 50 cGy irradiated mice compared with controls ($P < 0.05$), and these effects were mitigated by ALA supplementation.

At 6 h after irradiation, NTY immunostaining in oocytes was significantly increased among groups for primordial and secondary follicles ($P < 0.05$, Fig. 5D), while staining in granulosa cells was not ($P > 0.05$, Fig. 5C). The percentages of primordial and secondary follicles with NTY-positive oocytes were significantly higher in 50 cGy exposed mice compared with 0 cGy controls ($P < 0.05$, Fig. 5D), and these effects were mitigated by ALA supplementation (Fig. 5). At 1 week after irradiation, NTY staining did not vary significantly among the groups (Fig. 5E and F).

Charged iron particles increase ovarian follicular apoptosis

We quantified the percentages of follicles undergoing apoptosis at 6 h and 1 week post-irradiation using activated (cleaved) caspase-3 and PUMA (pro-apoptotic BCL-2 family member) immunostaining (Figs 6 and 7). At 6 h after irradiation, the percentage of secondary follicles with activated caspase 3-positive granulosa cells was significantly elevated in the 50 cGy iron compared with the 0 cGy group ($P < 0.05$; Fig. 6C), and ALA supplementation mitigated the effect. At 1 week after irradiation, the percentages of primordial and primary follicles with activated caspase 3-positive oocytes and the percentage of secondary follicles with activated caspase 3 positive granulosa cells were significantly elevated in the 50 cGy iron compared with the 0 cGy group ($P < 0.05$; Fig. 6E and F), and ALA supplementation mitigated these effects.

Because acute increases in PUMA are required for γ-radiation-induced germ cell death in neonatal ovaries (Kerr *et al.*, 2012), we analyzed the expression of PUMA in the ovary at 6 h after iron irradiation in the 0, 50 and 50 cGy plus ALA groups (Fig. 7). The percentages of secondary and antral follicles with PUMA-positive granulosa cells were

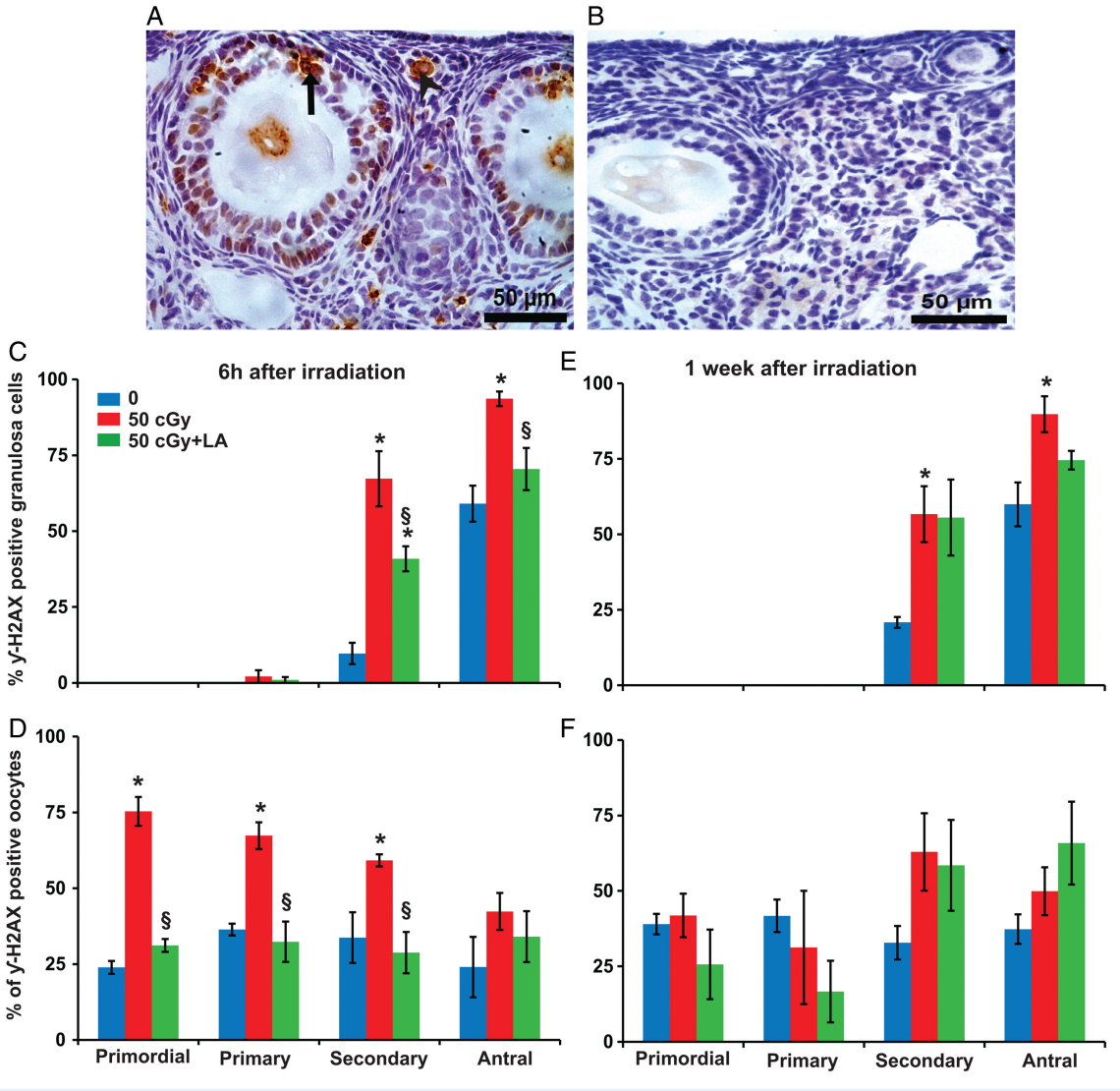

Figure 3 Charged iron particles increase ovarian γH2AX immunostaining. Representative image of γH2AX immunostaining in granulosa cells (black arrow) and oocytes (arrowhead) of follicles (**A**), and negative control image with primary antibody replaced by nonimmune IgG (**B**). Graphs show the mean ± SEM percentage of follicles with γH2AX-positive granulosa cells or oocytes. (**C**) Six hours after irradiation, there were statistically significant differences in percentages of secondary and antral follicles with γH2AX-positive granulosa cells among groups ($P < 0.05$, Kruskal–Wallis tests). (**D**) At 6 h there were statistically significant differences in percentages of primordial, primary and secondary follicles with γH2AX-positive oocytes ($P < 0.05$, Kruskal–Wallis tests). (**E**) One week after irradiation, there were statistically significant differences in percentages of secondary and antral follicles with γH2AX-positive granulosa cells among groups ($P < 0.05$, Kruskal–Wallis tests). (**F**) At 1 week, there were no statistically significant differences in percentages of follicles with γH2AX-positive oocytes among groups. *$P < 0.05$ versus 0 cGy control by Mann–Whitney test; §$P < 0.05$, 50 cGY + ALA versus 50 cGy by Mann–Whitney test. $n = 4$ mice/group.

significantly elevated in mice treated with 50 cGy iron compared with 0 cGy ($P < 0.05$; Fig. 7C). The percentages of primordial, primary, and secondary follicles with PUMA-positive oocytes were significantly higher in 50 cGy irradiated mice compared with controls (Fig. 7D). All of these effects were mitigated by ALA supplementation.

Charged iron particles do not alter ovarian cell proliferation

To determine whether 50 cGy iron irradiation affects granulosa cell proliferation, we analyzed the expression of PCNA, a marker for proliferating cells, at 6 h after irradiation. The percentages of follicles with PCNA-positive granulosa cells (Supplementary data, Fig. S1C) or oocytes (Supplementary data, Fig. S1D) did not vary significantly among groups.

Discussion

The ovary is known to be highly sensitive to low LET γ-radiation, but our study is the first to quantify the effects of high-LET charged particles on ovarian follicles. It is important to understand the effects of charged

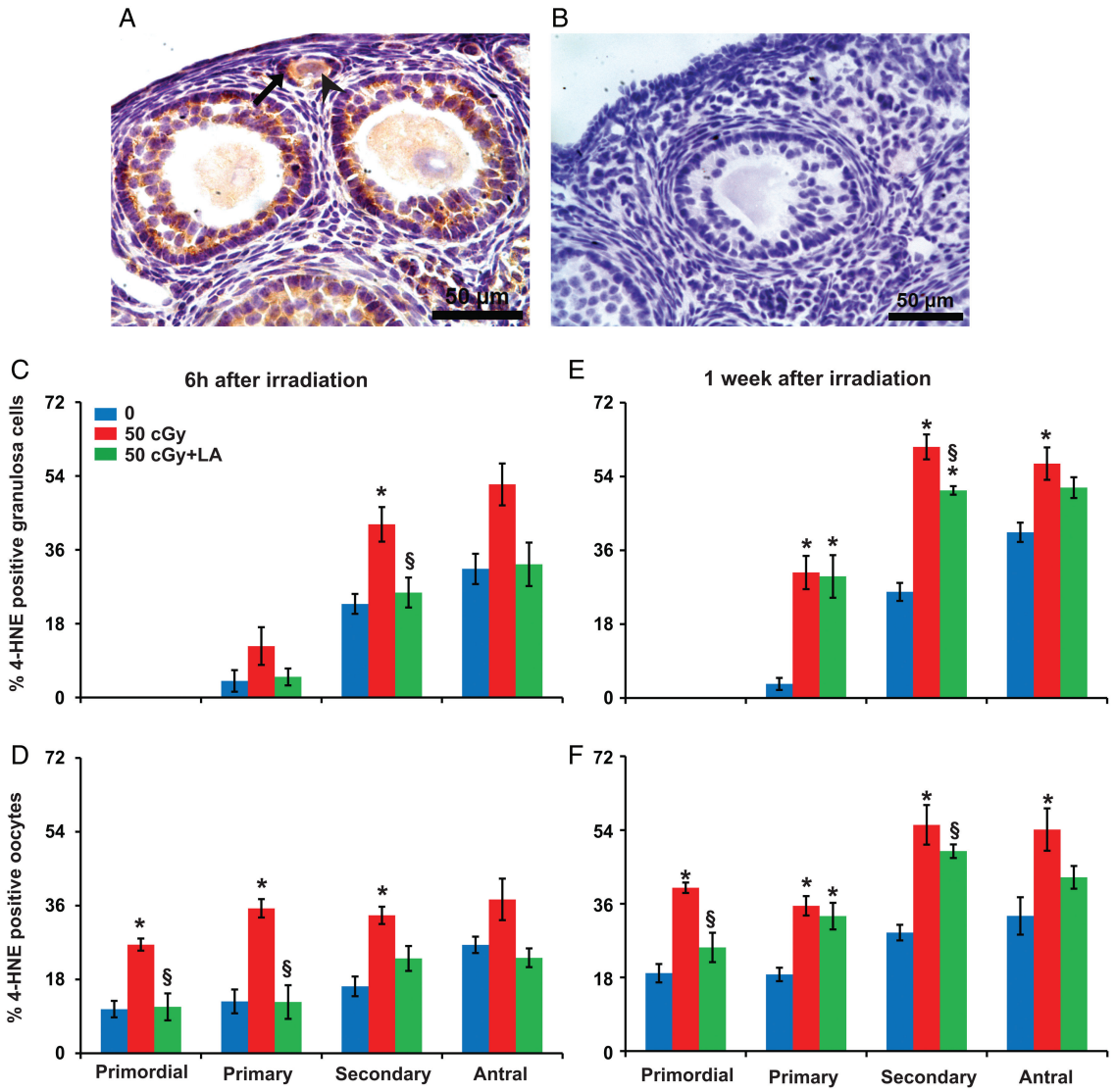

Figure 4 Charged iron particles increase lipid peroxidation in ovarian follicles. (**A**) Representative image of 4-HNE localization in granulosa cells (black arrow) and oocyte (arrowhead) of follicles. (**B**) Negative control with primary antibody replaced by nonimmune IgG. Graphs show the means ± SEM of percentages of follicles with 4-HNE positive granulosa cells or oocytes. (**C**) Six hours after irradiation, percentages of follicles with 4-HNE positive granulosa cells varied significantly among groups for secondary follicles ($P < 0.05$, Kruskal–Wallis test) and approached significance for antral follicles ($P = 0.08$). (**D**) Percentages of follicles with 4-HNE positive oocytes varied significantly among groups for primordial, primary and secondary follicles ($P < 0.05$, Kruskall–Wallis test) and approached significance for antral follicles ($P = 0.06$). (**E**) One week after irradiation, percentages of primary, secondary and antral follicles with 4-HNE positive granulosa cells varied significantly among groups ($P < 0.05$, Kruskal–Wallis test). (**F**) At 1 week, percentages of follicles with 4-HNE positive oocytes varied significantly among groups for primordial, primary, secondary and antral follicles ($P < 0.05$, Kruskal–Wallis test). *$P < 0.05$ versus 0 cGy control by Mann–Whitney test; §$P < 0.05$, 50 cGY + ALA versus 50 cGy by Mann–Whitney test. $n = 4$ mice/group.

particles on the ovary because of their increasing use in cancer therapy and because astronauts are exposed to charged particles. Our results reveal that acute exposure to charged iron particles increases γH2AX immunostaining, oxidative stress and apoptosis in ovarian follicles, resulting in depletion of ovarian follicles and decreased ovarian negative feedback to the hypothalamus and pituitary. Ovarian follicle numbers were dose-dependently depleted at 1-week post-irradiation, with further declines at 8 weeks. At 8 weeks, the primordial follicle reserve was decreased by 57% at the lowest dose of 5 cGy and was 99% depleted at the 50 cGy dose. Our results further demonstrate that dietary supplementation with the antioxidant ALA partially protects against the ovarian damage of charged iron particles, but does not prevent the near-complete depletion of primordial follicles in mice irradiated with 50 cGy iron.

The dose–response we observed for the depletion of primordial ovarian follicles in response to charged iron particles shows an ED_{50} at 8 weeks after irradiation of ~5 cGy. Previous studies in mice have not used doses as low as 5 cGy, but whole body irradiation with 50 or 60 cGy γ-radiation reportedly depleted >60% of ovarian follicles in adult Swiss albino and C57BL/CDA F1 hybrid mice (Mathur *et al.*,

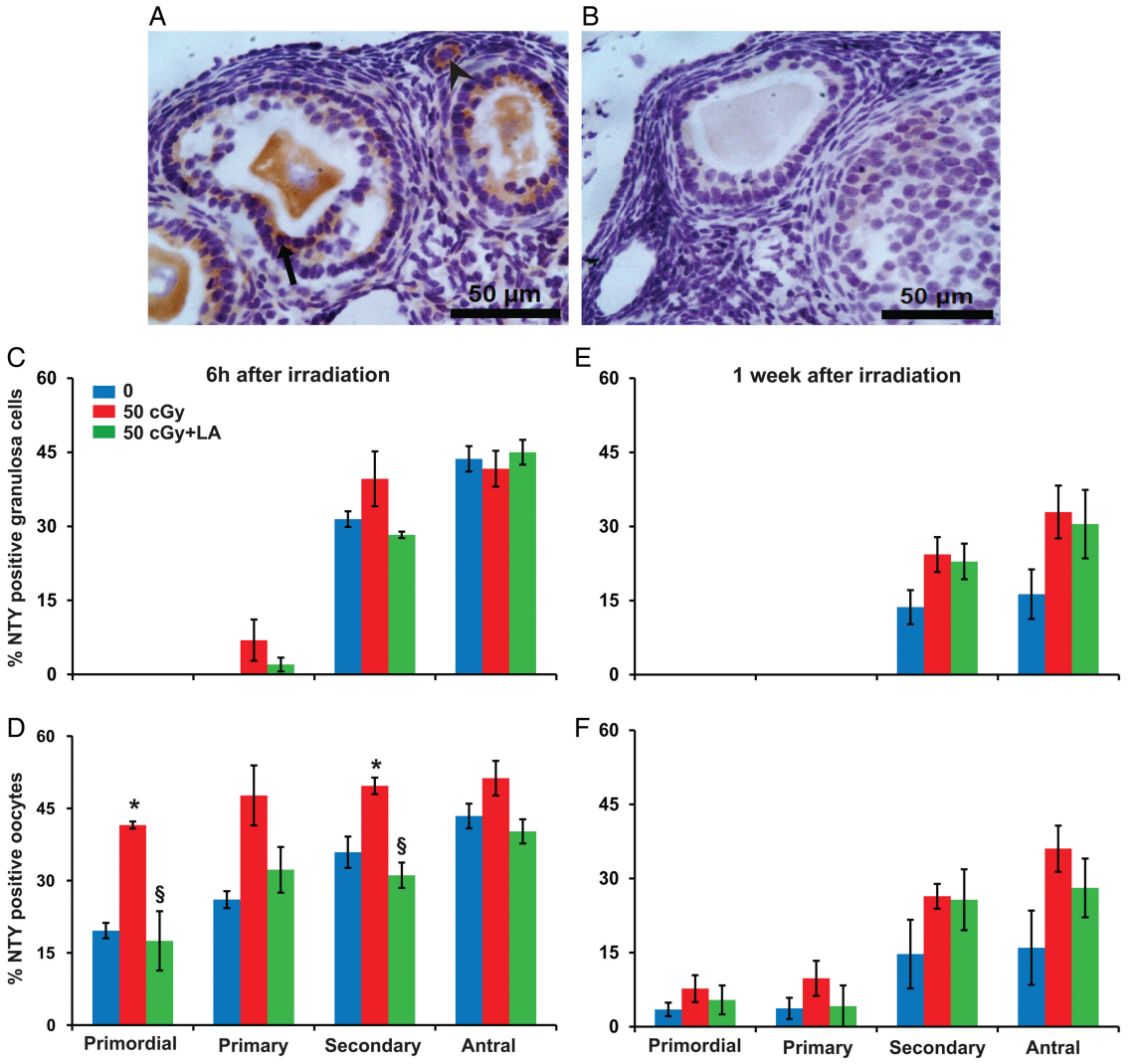

Figure 5 Charged iron particles increase protein nitration in ovarian follicles. (**A**) Representative image of NTY localization in granulosa cells (black arrow) and oocytes (arrowhead) of follicles. (**B**) Negative control image with primary antibody replaced by nonimmune IgG. Graphs show the mean ± SEM percentage of follicles with NTY-positive granulosa cells or oocytes; 6 h after irradiation, NTY immunostaining in granulosa cells did not vary among groups ($P > 0.05$, Kruskal–Wallis test) (**C**), while percentages of primordial and secondary follicles with NTY-positive oocytes varied significantly among groups ($P < 0.05$, Kruskall–Wallis test) (**D**). One week after irradiation, percentages of follicles with NTY-positive granulosa cells (**E**) and percentages of follicles with NTY-positive oocytes did not vary among groups ($P > 0.05$, Kruskal–Wallis test). *$P < 0.05$ versus 0 cGy control by Mann–Whitney test; §$P < 0.05$, 50 cGY + ALA versus 50 cGy by Mann–Whitney test. $n = 4$ mice/group.

1991; Pesty *et al.*, 2009), which is similar to the 84% depletion we observed at 30 cGy. In women, the ED_{50} for γ-radiation has been estimated at <2 Gy (Wallace *et al.*, 2003). Irradiation of mice with charged iron particles significantly and dose-dependently increased serum FSH concentrations and LH concentrations, consistent with decreased ovarian negative feedback due to depletion of ovarian follicles.

Ionizing radiation causes direct DNA damage, but generation of ROS from indirect ionization of water is thought to account for the majority of DNA damage caused by radiation (Spitz *et al.*, 2004; Dayal *et al.*, 2008). DNA double strand breaks can be induced by direct action of radiation on DNA and can also result from oxidative DNA lesions (Cadet *et al.*, 2012). Increased ROS persist for days and even weeks after ionizing radiation exposure (Spitz *et al.*, 2004; Dayal *et al.*, 2008). We previously showed that ROS increased in human COV434 granulosa cells within 30 min after γ-irradiation and persisted for at least 2 days, whereas overexpression of glutamate cysteine ligase subunits to enhance glutathione synthesis prevented the radiation-induced rise in ROS and apoptotic cell death (Cortés-Wanstreet *et al.*, 2009). Our data are consistent with the hypothesis that oxidative stress mediates the induction of apoptotic destruction of ovarian follicles by charged iron particles. We observed increased oxidative lipid and/or protein damage at 6 h and 1 week after irradiation, as well as γH2AX immunostaining, in oocytes and granulosa cells of ovarian follicles. Further supporting a mechanistic role of oxidative stress, supplementation with the antioxidant ALA mitigated some ovarian effects of charged iron particles. Previous studies have shown that ALA supplementation increases cellular uptake of

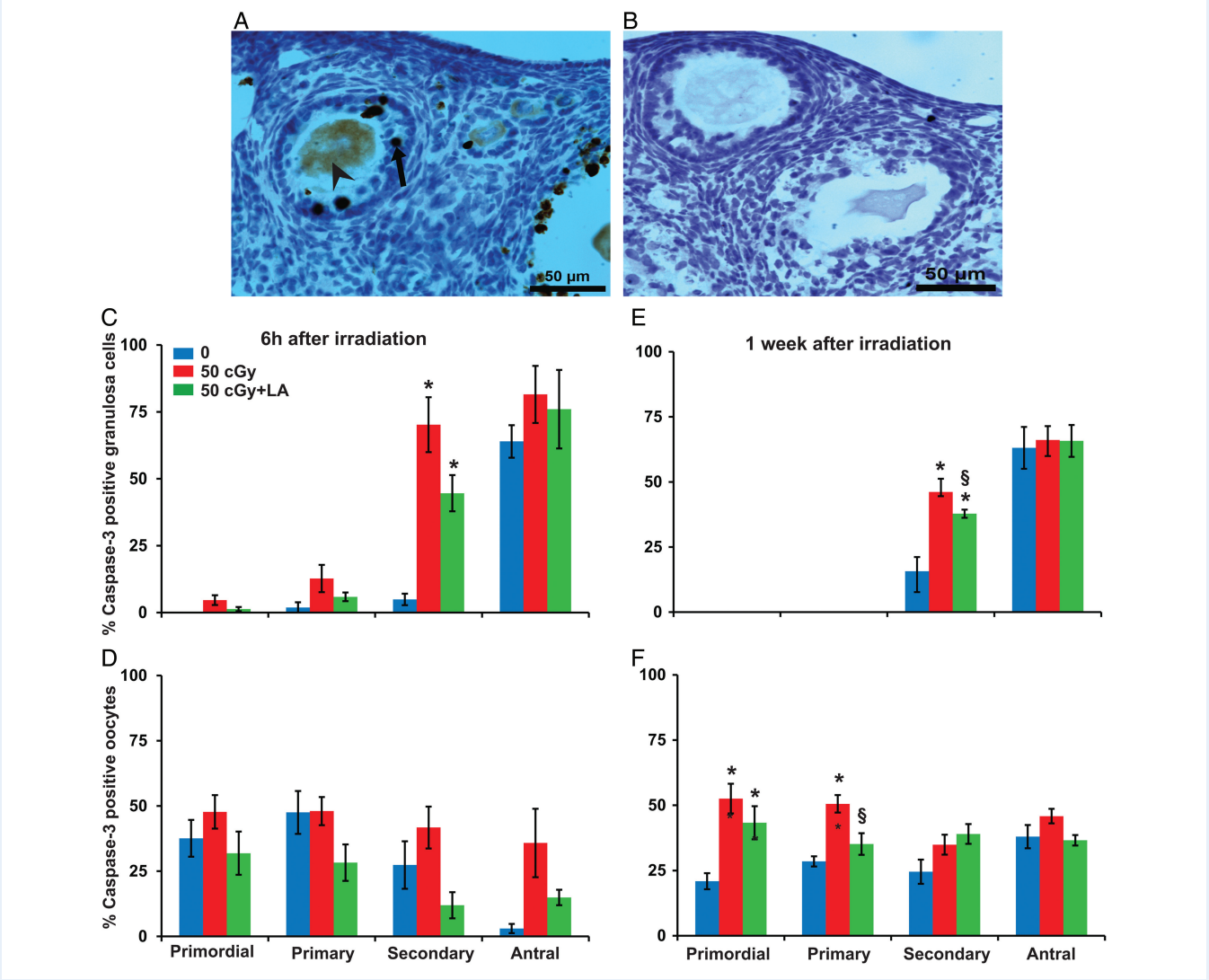

Figure 6 Charged iron particles increase caspase-3 activation in ovarian follicles. (**A**) Representative image of activated caspase-3 localization in granulosa cells (black arrow) and oocytes (arrowhead) of follicles. (**B**) Negative control with primary antibody replaced by nonimmune IgG. Graphs show the means ± SEM percentages of follicles with caspase-3 positive granulosa cells or oocytes. (**C**) At 6 h after irradiation, the effect of treatment group on percentages of follicles with caspase 3-positive granulosa cells approached significance for primordial follicles ($P = 0.07$, Kruskal–Wallis test) and was statistically significant for secondary follicles ($P < 0.05$, Kruskal–Wallis test). (**D**) Caspase-3 immunostaining in oocytes did not vary among groups at 6 h. (**E**) One week after irradiation, the percentage of secondary follicles with activated caspase 3-positive granulosa cells varied significantly among groups ($P < 0.05$, Kruskal–Wallis test). (**F**) One week after irradiation, percentages of primordial and primary follicles with activated caspase 3 positive oocytes varied significantly among groups ($P < 0.05$, Kruskal–Wallis test). $^{*}P < 0.05$ versus 0 cGy control by Mann–Whitney test; $^{\S}P < 0.05$, 50 cGY + ALA versus 50 cGy by Mann–Whitney test. $n = 4$ mice/group.

ascorbic acid and cysteine, increases translation of the transcription factor NRF2, which up-regulates antioxidant genes, and is protective against some effects of ionizing radiation (Suh *et al.*, 2004; Limoli *et al.*, 2007; Petersen Shay *et al.*, 2009, 2012). Similar to our observations, ALA was only partially protective against the effects of charged particles on bone (Schreurs *et al.*, 2016).

The pro-apoptotic BH3-only BCL-2 family protein PUMA is required for germ cell apoptosis induction by γ-radiation in neonatal ovaries (Kerr *et al.*, 2012). We similarly observed significant increases in PUMA immunostaining in oocytes of primordial, primary and secondary follicles 6 h post-irradiation. Both PUMA and caspase 3 activation were increased in granulosa cells of secondary follicles at 6 h. No increase in caspase 3 activation was observed in oocytes of follicles at 6 h; however, caspase-3 activation was increased in oocytes of primordial and primary follicles at 1 week after irradiation. It is possible that the initial peak of caspase 3 activation occurred between the 6 h and 1 week time points in the present study, as a previous study reported that the peak of oocyte apoptosis occurs 12 h after high-LET neutron irradiation (Nitta and Hoshi, 2003).

Accelerated recruitment of primordial follicles into the growing pool, followed by apoptotic death at later stages of follicular development, has been recognized as an important pathway leading to premature ovarian failure due to genetic modifications (Zheng *et al.*, 2012) or exposure to

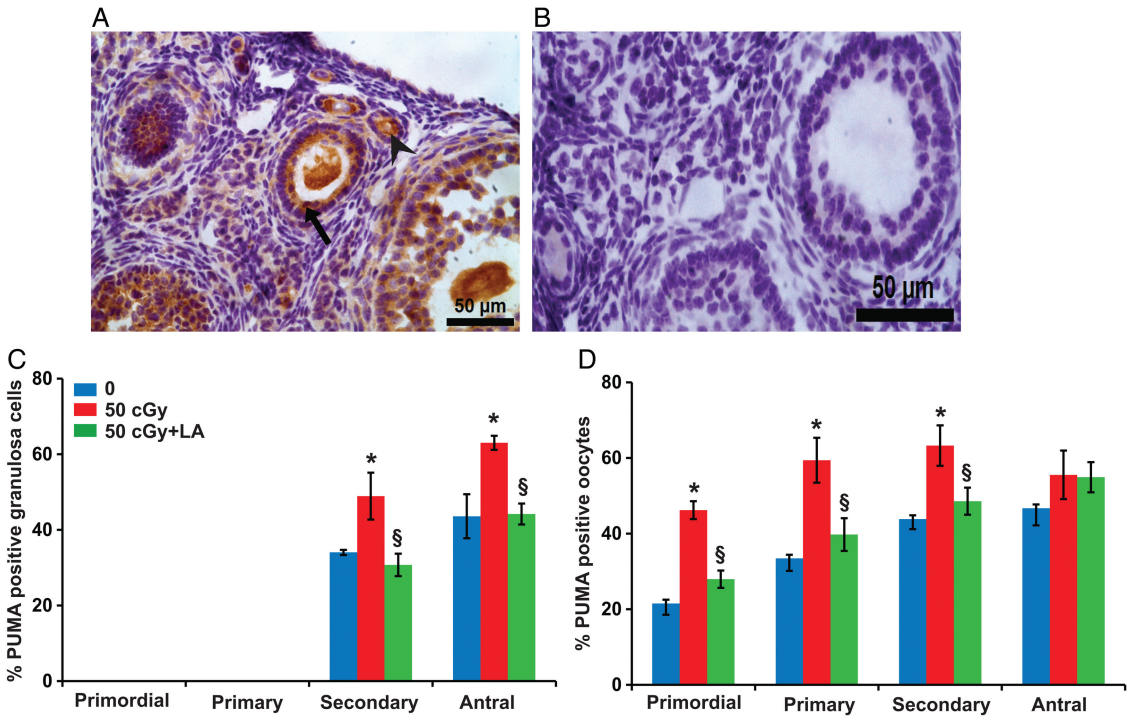

Figure 7 Induction of apoptosis in ovarian follicles by charged iron particles involves PUMA. (**A**) Representative image of PUMA localization in granulosa cells (black arrow) and oocytes (arrowhead) of follicles. (**B**) Negative control image with primary antibody replaced by nonimmune IgG. Graphs show the means ± SEM of percentages of follicles with PUMA-positive granulosa cells or oocytes at 6 h after irradiation. (**C**) Percentages of secondary and antral follicles with PUMA-positive granulosa cells varied significantly among groups ($P < 0.05$, Kruskal–Wallis test). (**D**) Percentages of primordial, primary, and secondary follicles with PUMA-positive oocytes varied significantly among groups ($P < 0.05$, Kruskal–Wallis test). *$P < 0.05$ versus 0 cGy control by Mann–Whitney test; §$P < 0.05$, 50 cGY + ALA versus 50 cGy by Mann–Whitney test. $n = 4$ mice/group.

toxicants (Sobinoff *et al.*, 2012). We observed no effects of charged iron on immunostaining for the proliferation marker PCNA in follicles of any stage at 6 h after irradiation. Our results contrast with reportedly decreased PCNA staining in granulosa cells of follicles 4 days after irradiation of rats with 3.2 Gy γ-rays (Mahran *et al.*, 2013). Multiple differences between the studies could explain the divergent effects of radiation on follicular proliferation, including different time points examined, type of radiation and species studied. Taken together, our results suggest that primordial follicle depletion by charged iron particle irradiation is more likely caused by direct destruction than increased recruitment of primordial follicles.

In conclusion, our results show that a 5 cGy dose of charged iron particle radiation, which is 8-fold lower than the estimated cumulative dose during a Mars mission, decreases the primordial follicle pool by more than half, while a 50 cGy dose, which is slightly more than the estimated dose from a Mars mission, depletes primordial follicles by 99%. Our results further show that exposure to 50 cGy charged iron particles increases γH2AX immunostaining, oxidative protein and lipid damage, and apoptosis in ovarian follicles via a pathway involving up-regulation of the proapoptotic BCL-2 family protein PUMA and caspase 3 activation. Although we did not examine the latter end-points at lower doses, we believe it is likely that the same mechanistic pathway is activated, albeit to a lesser extent at lower doses, culminating in dose- and time-dependent depletion of the primordial follicle pool and premature ovarian failure. Finally, our results show that ALA supplementation is partially protective against ovarian effects of charged iron particles, but is insufficient as a single agent to prevent follicle depletion.

Supplementary data

Supplementary data are available at http://humrep.oxfordjournals.org/.

Acknowledgements

The authors thank Drs Peter Guida, Chiara La Tessa and Adam Rusek, and staff at the NASA Space Radiation Laboratory for their support.

Authors' roles

B.M. collected samples, conducted experiments, analyzed data and drafted the manuscript. L.O. assisted in conducting experiments. U.L. designed the study, assisted in conducting experiments, analyzed data and drafted the manuscript.

Funding

This study was supported by a National Aeronautics and Space Administration grant NNX14AC50G to U.L.; National Institutes of Health grant P30CA062203 for the University of California Irvine (UC Irvine) Chao Family Comprehensive Cancer Center; the Center for

Occupational and Environmental Health, UC Irvine; the University of Virginia Center for Research in Reproduction Ligand Assay and Analysis Core funded by the Eunice Kennedy Shriver NICHD/NIH (NCTRI) grant P50-HD28934. B.M. was partially supported by a First award fellowship from the National Space Biomedical Research Institute grant PF04302.

Conflict of interest

None declared.

References

Barcellus-Hoff MH, Blakely EA, Burma S, Fornace AJJ, Gerson S, Hlatky L, Kirsch DG, Luderer U, Shay J, Wang Y *et al*. Concepts and challenges in cancer risk prediction for the space radiation environment. *Life Sci Space Res* 2015;**6**:92–103.

Cadet J, Ravanat J-L, TavernaPorro M, Menoni H, Angelov D. Oxidatively generated complex DNA damage: tandem and clustered lesions. *Cancer Lett* 2012;**327**:5–15.

Canning J, Takai Y, Tilly JL. Evidence for genetic modifiers of ovarian follicular endowment and development from studies of five inbred mouse strains. *Endocrinology* 2002;**144**:9–12.

Capen CC, Beamer WG, Tennent BJ, Stitzel KA. Mechanisms of hormone-mediated carcinogenesis in the ovary of mice. *Mutat Res* 1995;**333**:143–151.

Cooper RL, Goldman JM, Vandenbergh JG. Monitoring of the estrous cycle in the laboratory rodent by vaginal lavage. In: Heindel JJ, Chapin RE (eds). *Female Reproductive Toxicology, Methods in Toxicology, Vol. 3b*. San Diego: Academic Press, Inc., 1993,45–55.

Cortés-Wanstreet MM, Giedzinski E, Limoli CL, Luderer U. Overexpression of glutamate cysteine ligase protects human COV434 granulosa tumor cells against oxidative and γ-radiation-induced cell death. *Mutagenesis* 2009;**24**:211–224.

Cucinotta FA, Durante M. Cancer risk from exposure to galactic cosmic rays: implications for space exploration by human beings. *Lancet Oncol* 2006; **7**:431–435.

Dayal D, Martin SM, Limoli CL, Spitz DR. Hydrogen peroxide mediates the radiation-induced mutator phenotype in mammalian cells. *Biochem J* 2008;**413**:185–191.

Devine PJ, Perreault SD, Luderer U. Roles of reactive oxygen species and antioxidants in ovarian toxicity. *Biol Reprod* 2012;**86**:1–10.

Gosden RG, Laing SC, Felicio LS, Nelson JF, Finch CE. Imminent oocyte exhaustion and reduced follicular recruitment mark the transition to acyclicity in aging C57BL/6J mice. *Biol Reprod* 1983;**28**:255–260.

Hirshfield AN. Size-frequency analysis of Atresia in cycling rats. *Biol Reprod* 1988;**38**:1181–1188.

Hirshfield AN. Overview of ovarian follicular development: considerations for the toxicologist. *Environ Mol Mutagen* 1997;**29**:10–15.

Kerr JB, Hutt KJ, Michalak EM, Cook M, Vandenberg CJ, Liew SH, Bouillet P, Mills A, Scott CL, Findlay JK *et al*. DNA damage-induced primordial follicle oocyte apoptosis and loss of fertility require TAp63-mediated induction of PUMA and NOXA. *Mol Cell* 2012;**48**:343–352.

Kim JK, Lee CJ. Effect of exogenous melatonin on the ovarian follicles in ϒ-irradiated mouse. *Mutat Res* 2000;**449**:33–39.

Lee CJ, Yoon Y-D. ϒ-Radiation-induced follicular degeneration in the prepubertal mouse ovary. *Mutat Res* 2005;**578**:247–255.

Lee CJ, Park HH, Do BR, Yoon YD, Kim JK. Natural and radiation-induced degeneration of the primordial and primary follicles in the mouse ovary. *Anim Reprod Sci* 2000;**59**:109–117.

Lim J, Lawson GW, Nakamura BN, Ortiz L, Hur JA, Kavanagh TJ, Luderer U. Glutathione-deficient mice have increased sensitivity to transplacental benzo[a]pyrene-induced premature ovarian failure and ovarian tumorigenesis. *Cancer Res* 2013;**73**:908–917.

Lim J, Nakamura BN, Mohar I, Kavanagh TJ, Luderer U. Glutamate cysteine ligase modifier subunit (Gclm) null mice have increased ovarian oxidative stress and accelerated age-related ovarian failure. *Endocrinology* 2015; **156**:3329–3343.

Limoli CL, Giedzinski E, Baure J, Rola R, Fike JR. Redox changes induced in hippocampal precursor cells by heavy ion irradiation. *Radiat Environ Biophys* 2007;**46**:167–172.

Loeffler JS, Durante M. Charged particle therapy - optimization, challenges, and future directions. *Nat Rev Clin Oncol* 2012;**10**:411–424.

Lopez SG, Luderer U. Effects of cyclophosphamide and buthionine sulfoximine on ovarian glutathione and apoptosis. *Free Radic Biol Med* 2004;**36**:1366–1377.

Mahran YF, El-Demerdash E, Nada AS, Ali AA, Abdel-Naim AB. Insights into the protective mechanisms of tamoxifen in radiotherapy-induced ovarian follicular loss: impact on insulin-like growth factor 1. *Endocrinology* 2013; **154**:3888–3899.

Mathur S, Nandchahal K, Bhartiya HC. Radioprotection by MPG of mice ovaries exposed to sublethal gamma radiation doses at different postnatal ages. *Acta Oncol* 1991;**30**:981–983.

Meirow D, Nugent D. The effects of radiotherapy and chemotherapy on female reproduction. *Hum Reprod Update* 2001;**7**:535–543.

Molina JR, Barton DL, Loprinzi CL. Chemotherapy-induced ovarian failure. Manifestations and management. *Drug Saf* 2005;**28**:401–416.

Nitta Y, Hoshi M. Relationship between oocyte apoptosis and ovarian tumors induced by high and low LET radiations in mice. *Int J Radiat Biol* 2003;**79**:241–250.

Pesty A, Doussau M, Lahaye J-B, Lefèvre B. Whole-body or isolated ovary 60Co irradiation: effects on in vivo and in vitro folliculogenesis and oocyte maturation. *Reprod Toxicol* 2009;**29**:93–98.

Petersen Shay K, Moreau RF, Smith EJ, Smith AR, Hagen TM. Alpha-lipoic acid as a dietary supplement: molecular mechanisms and therapeutic potential. *Biochim Biophys Acta* 2009;**1790**:1149–1160.

Petersen Shay K, Michels AJ, Li W, Kong A-NT, Hagen TM. Cap-independent Nrf2 translation is part of a lipoic acid-stimulated detoxification stress response. *Biochim Biophys Acta* 2012;**1823**:1102–1109.

Radi R. Peroxynitrite, a stealthy biological oxidant. *J Biol Chem* 2013; **288**:26464–26472.

Reeg S, Grune T. Protein oxidation in aging: does it play a role in aging progression? *Antiox Redox Signal* 2015;**23**:239–255.

Roede JR, Jones DP. Reactive species and mitochondrial dysfunction: mechanistic significance of 4-hydroxynonenal. *Environ Mol Mutagen* 2010;**51**:380–390.

Ronca AE, Baker ES, Bavendam TG, Beck KD, Miller VM, Tash JS, Jenkins M. Effects of sex and gender on adaptations to space: reproductive health. *J Womens Health* 2014;**23**:967–974.

Schreurs A-S, Shirazi-Fard Y, Shahnazari M, Alwood JS, Truong TA, Tahimic CGT, Limoli CL, Turner ND, Halloran B, Globus RK. Dried plum diet protects from bone loss caused by ionizing radiation. *Sci Rep* 2016;**6**:21343.

Shuster LT, Gostout BS, Grossardt BR, Rocca WA. Prophylactic oophorectomy in premenopausal women and long-term health. *Menopause Int* 2008;**14**:111–116.

Silva I, Mor G, Naftolin F. Estrogen and the aging brain. *Maturitas* 2001; **38**:95–100.

Slaba TC, Blattnig SR, Norbury JW, Rusek A, La Tessa C, Walker SA. *GCR Simulator Reference Field and A Spectral Approach for Laboratory Simulation NASA Technical Publication*. Langley, VA: NASA, 2015.

Sobinoff AP, Pye V, Nixon B, Roman SD, McLaughlin EA. Jumping the gun: smoking constituent BaP causes premature primordial follicle activation and impairs oocyte fusibility through oxidative stress. *Toxicol Appl Pharmacol* 2012;**260**:70–80.

Spitz DR, Azzam EI, Li JJ, Gius D. Metabolic oxidation/reduction reactions and cellular response to ionizing radiation: a unifying concept in stress response biology. *Cancer Metastasis Rev* 2004;**23**:311–322.

Sridharan DM, Chappell LJ, Whalen MK, Cucinotta FA, Pluth JM. Defining the biological effectiveness of components of high-LET track structure. *Radiat Res* 2015;**184**:105–119.

Suh JH, Shenvi SV, Dixon BM, Liu H, Jaiswal AK, Liu R-M, Hagen TM. Decline in transcriptional activity of Nrf2 causes age-related loss of glutathione synthesis, which is reversible with lipoic acid. *Proc Natl Acad Sci USA* 2004;**101**:3381–3386.

Svejme O, Ahlborg HG, Nilsson J-Å, Karlsson MK. Early menopause and risk of osteoporosis, fracture and mortality: a 34-year prospective observational study in 390 women. *BJOG* 2012;**119**:810–816.

Tokuyama Y, Furusawa Y, Ide H, Yasui A, Terato H. Role of isolated and clustered DNA damage and the post-irradiating repair process in the effects of heavy ion beam irradiation. *J Radiat Res (Tokyo)* 2015; **56**:446–455.

Tsai-Turton M, Luderer U. Opposing effects of glutathione depletion and FSH on reactive oxygen species and apoptosis in cultured preovulatory rat follicles. *Endocrinology* 2006;**147**:1224–1236.

Tsai-Turton M, Nakamura BN, Luderer U. Induction of apoptosis by 9,10-dimethyl-1,2-benzanthracene (DMBA) in cultured preovulatory rat follicles is preceded by a rise in reactive oxygen species and is prevented by glutathione. *Biol Reprod* 2007;**77**:442–451.

Vanderhyden BC, Shaw TJ, Ethier J-F. Animal models of ovarian cancer. *Reprod Biol Endocrinol* 2003;**1**:67.

Wallace WHB, Shalet SM, Hendry JH, Morris-Jone PH, Gattamaneni HR. Ovarian failure following abdominal irradiation in childhood: the radiosensitivity of the human oocyte. *Br J Radiol* 1989;**62**:995–998.

Wallace WHB, Thomson AB, Kelsey TW. The radiosensitivity of the human oocyte. *Hum Reprod* 2003;**18**:117–121.

Zheng W, Nagaraju G, Liu Z, Liu K. Functional roles of the phosphatidylinositol 3-kinases (PI3Ks) signaling in the mammalian ovary. *Mol Cell Endocrinol* 2012;**356**:24–30.